

Microwave Properties of MgB₂ Thin Films

N. Klein, B. B. Jin, R. Wördenweber, P. Lahl, W. N. Kang, Hyeong-Jin Kim, Eun-Mi Choi, Sung-IK Lee, T. Dahm, and K. Maki

Abstract—The microwave surface impedance $Z_s = R_s + j\omega\mu_0\lambda$ of MgB₂ thin films was measured via advanced dielectric resonator (DR) techniques. First, the temperature dependence of the penetration depth λ measured with a sapphire puck at 17.9 GHz can be well fitted from 5 K close to T_c by the standard BCS integral expression assuming the reduced energy gap $\Delta(0)/kT_c$ to be as low as 1.0–1.1 assuming $\lambda(0) = 100$ –110 nm. These results clearly indicate the s-wave nature of the order parameter. Similar good fits were achieved by an anisotropic one gap and an isotropic two-gap model. Second, the temperature dependence of surface resistance R_s , as measured with a rutile puck, indicates an exponential behavior below about $T_c/2$ with a reduced energy gap being consistent with the one determined from the λ data. The R_s value at 4.2 K was found to be as low as 19 $\mu\Omega$ at 7.2 GHz, which is comparable with that of a high-quality high temperature thin films of YBa₂Cu₃O₇. A higher-order mode at 17.9 GHz was employed to investigate the frequency f dependence of $R_s\alpha f^{n(T)}$. Our results revealed an decrease of n with increasing temperature ranging from $n = 2$ below 8 K to $n = 1$ close to T_c . Finally, the microwave power handling of MgB₂ films was deduced and compared with values for YBa₂Cu₃O₇ films. We found that the power handling of MgB₂ is comparable or even better than that of YBa₂Cu₃O₇ films for temperature below 30 K.

Index Terms—Energy gap, microwave measurement, penetration depth, superconducting films.

I. INTRODUCTION

THE discovery of superconductivity in magnesium diboride has stimulated extensive theoretical and experimental studies on this material [1]–[18]. Microwave measurements of the surface impedance $Z_s = R_s + jX_s$, where R_s is the surface resistance and X_s the surface reactance, play an important role in understanding the physics and in finding potential applications of this material [15]–[18]. X_s is proportional to penetration depth λ , which is related to the superconducting electron density and can provide information on order parameter symmetry [19]. Microwave measurements have proved to be the most sensitive tool to determine the temperature dependence of λ of both thin film and bulk single crystal samples of

HTS [19]–[22], and are therefore most appropriate to be used for high-precision $\lambda(T)$ measurements on high quality MgB₂ samples [15], [16].

For a superconductor R_s is proportional to the conductivity of thermally excited quasiparticles. The s-wave nature of the order parameter of MgB₂ suggests an exponential temperature dependence of R_s in the low temperature region (below about 20 K) [15], [17], [18], if the impurity and defect related residual surface resistance $R_s(T \rightarrow 0)$ is low enough. In contrast to oxide superconductors, grain boundaries do not exhibit weak link behavior, i.e., one important potential source of extrinsic residual losses is expected not to be present. However, the presence of a small energy gap is expected to cause high intrinsic losses by quasiparticle absorption down to relatively low temperatures. Therefore, a careful study of the surface impedance is necessary to judge whether this material may become a possible candidate of replacement of Nb or Nb alloys for cavity applications.

II. SAMPLE PREPARATION AND MEASUREMENT TECHNIQUES

MgB₂ thin films were deposited by pulsed laser deposition and post-annealing on a plane parallel [1 $\bar{1}$ 02] oriented sapphire substrate of 10 \times 10 mm² in size. The samples exhibit a sharp resistive and inductive transition at transition temperatures up to 39 K (onset temperature of resistive transition). The detailed process is described in [23]. The film thickness was 400 nm. X-ray diffraction analysis indicates a high degree of c -axis-orientation perpendicular to the substrate surface and no detectable amount of MgO or any other crystalline impurity phases.

The microwave surface impedance was determined using a dielectric resonator technique [24], [25]. The sample is placed underneath a dielectric puck. The resonant mode (commonly TE_{01 δ} mode) is excited by coaxial loops as transmission resonator. The unloaded quality factor Q_0 and resonant frequency f were recorded as a function of temperature. The temperature dependence of the variation of the effective penetration depth ($\delta\lambda^{\text{eff}}$) and surface resistance (R_s^{eff}) were determined from the temperature dependence of the resonant frequency $f(T)$ and unloaded quality factor $Q_0(T)$. The notation effective represents an enhancement of λ due to the thickness being of the order of λ [26].

A sapphire puck is employed to measure $\delta\lambda^{\text{eff}}$ because of the low temperature coefficient of its dielectric constant. The TE_{01 δ} mode of the puck at a frequency of 17.9 GHz is excited. There are possible parasitic contributions to change f apart from the change of penetration depth of the sample. The measurement shows that these contributions are at least one order of magnitude lower than the observed frequency changes of λ for our MgB₂ samples except for temperatures close to T_c [16]. Therefore, these contributions are neglected in our calculations.

Manuscript received August 7, 2002. This work was supported by the Ministry of Science and Technology of Korea through the Creative Research Initiative Program.

N. Klein, B. B. Jin, R. Wördenweber and P. Lahl are with Forschungszentrum Jülich, ISG, D-52425 Jülich, Germany (e-mail: n.klein@fz-juelich.de).

W. N. Kang, H.-J. Kim, E.-M. Choi and S.-I. Lee are with National Creative Research Initiative Center for Superconductivity, Department of Physics, Pohang University of Science and Technology, Pohang, 790-784, Republic of Korea.

T. Dahm is with Universität Tübingen, Institut für Theoretische Physik, Auf der Morgenstelle 14, 72076 Tübingen, Germany.

K. Maki is with Department of Physics and Astronomy, University of Southern California, Los Angeles, CA 90089-0484 USA.

Digital Object Identifier 10.1109/TASC.2003.812214

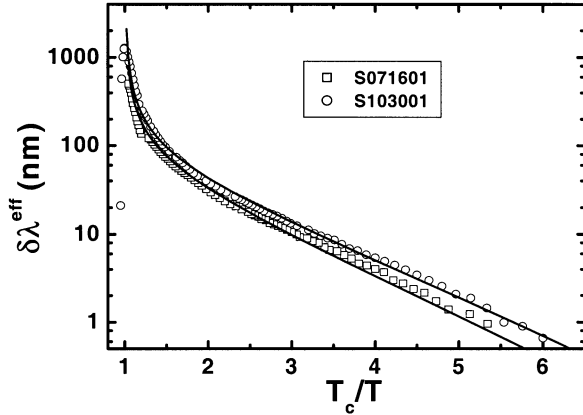


Fig. 1. $\log \delta\lambda^{\text{eff}}$ vs. T_c/T representation of the penetration depth data for two MgB_2 samples. The solid line represents BCS fits with parameters as described in the text.

The sapphire resonator mentioned above allows for the determination of R_s^{eff} with a systematic error of 0.1 m Ω , which is due to neglecting the temperature dependent background losses of the cavity and the finite microwave losses ($R_s \approx 10^{-5} \Omega$) of the Nb reference film. Indeed, MgB_2 seems to comprise R_s values of the order or less than this error margin, because Q_0 (4.2 K) for a MgB_2 was found almost to be the same as with niobium film. In order to improve the measurement resolution a rutile puck has been used to measure R_s^{eff} because of its higher dielectric constant [27], [28]. In this case the field energy concentration inside the puck works more effectively and the maximum Q_0 with a niobium reference sample is about a factor of ten higher. We have employed the $\text{TE}_{01\delta}$ mode at 7.18 GHz and the $\text{TE}_{41\delta}$ mode at 17.9 GHz to study temperature and frequency dependence of R_s .

III. PENETRATION DEPTH RESULTS

Two MgB_2 samples (S071 601 and S103001) were measured, and the results are depicted in Fig. 1 in a $\log \delta\lambda^{\text{eff}}$ versus T_c/T representation. It should be noted that the penetration depth studied here is in fact the penetration depth in a, b -plane (λ_{ab}) due to the c -axis orientation of the thin films. The nearly linear behavior in this semi-logarithmic plot clearly shows the existence of a full gap. Therefore, the symmetry of the order parameter is s-wave, which also has been found by other techniques [2]–[6], [13], [14].

A straightforward idea is to use BCS theory to explain the results. In the local limit the temperature dependence of λ can be calculated as follows:

$$\frac{1}{\lambda^2(T)} = \frac{1}{\lambda^2(0)} \left[1 - 2 \int_{\Delta(T)}^{\infty} -\frac{\partial f(\varepsilon)}{\partial \varepsilon} \frac{\varepsilon}{\sqrt{\varepsilon^2 - \Delta^2(T)}} d\varepsilon \right] \quad (1)$$

with $f(\varepsilon) = [\exp(\varepsilon/kT) + 1]^{-1}$ representing the Fermi function and $\Delta(T)$ the temperature dependence of energy gap [19]. The quantities $\Delta(0)/kT_c$ and $\lambda(0)$ are used as fit parameters. The parameters $\Delta(0)/kT_c = 1.13$, $\lambda(0) = 102$ m for sample S071 601 and $\Delta(0)/kT_c = 1.03$, and $\lambda(0) = 107$ m for sample S103001 yield a very good agreement between experimental data over the entire temperature range. However,

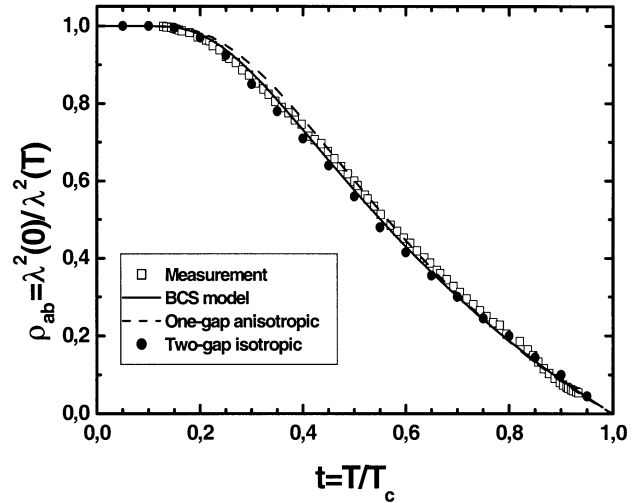


Fig. 2. $\lambda^2(0)/\lambda^2(T)$ dependence for the sample S071 601 (open square). The full lines represent BCS fits using $\Delta(0)/kT_c$ as fit parameter. The predictions by the one-gap anisotropic (dot line) and two-gap isotropic model (solid circle) are also drawn.

the low $\Delta(0)/kT_c$ (< 1.76 , BCS weak-coupling limit) is difficult to understand within a standard BCS type s-wave theory. Recently, theoretical and experimental evidences have shown that MgB_2 should be an isotropic two-gap [2], [4]–[8] or an anisotropic one-gap superconductor [3], [9], [10]. Thus, the small gap in our measurement represents the smallest component of a double or a strongly anisotropic gap. In this case the temperature dependence of λ at $T \ll T_c$ would be determined by its minimum values, because $\lambda(T)$ probes the thermal excitations with the lowest activation energy. Fig. 2 shows the temperature dependence of $\lambda^2(0)/\lambda^2(T)$ for sample S071 601 (open square), which represents the normalized superfluid density ρ_{ab} . As expected from Fig. 2, a very good agreement with single gap BCS theory (solid line) is achieved. However, the low $\Delta(0)/kT_c$ value determined from the fit may be regarded as a violation of BCS theory. Therefore, more advanced modeling is required.

Both an isotropic two-gap and an anisotropic one-gap BCS model have been used to explain our measurement. In the case of the one-gap anisotropic model an ellipsoidal energy gap function is assumed with a minor axis within the ab -plane and a major axis along c direction [9]. The temperature dependence of the gap and the gap ratios $\Delta_{\text{max}}(T=0)/kT_c$ and $\Delta_{\text{min}}(T=0)/kT_c$ are determined by a self-consistent solution of the anisotropic weak-coupling gap-equation with only one parameter $\gamma = \Delta_{\text{max}}/\Delta_{\text{min}}$. This model predicts that λ_{ab} is mainly determined by the small energy gap, which is consistent with our measurements. The dashed line in Fig. 2 represents the calculation with a maximum gap ratio $\Delta_{\text{max}}(T=0)/kT_c = 3.85$ and a minimum gap ratio $\Delta_{\text{min}}(T=0)/kT_c = 1.09$. However, the assumed energy gap anisotropy cannot explain upper critical field behavior, as discussed in [29].

A two-gap isotropic model has also been used to calculate the temperature dependence of λ_{ab} using the Eliashberg formalism and the results of first principles electronic structure calculation. The results are shown in Fig. 2 (solid dot). A very good agreement can be obtained if $\lambda_{ab}(0) = 39.2$ nm is assumed [11].

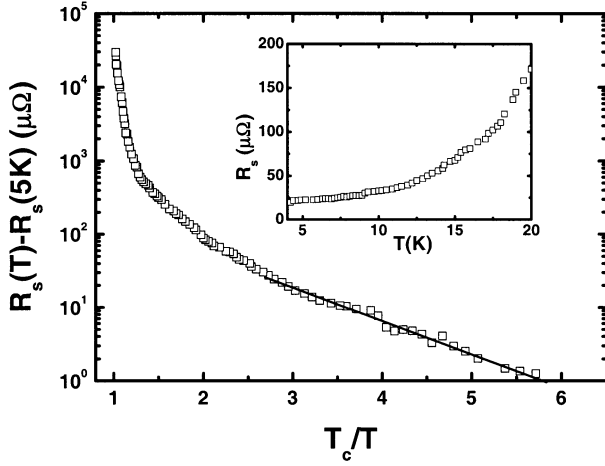


Fig. 3. $R_s(T) - R_s(5\text{ K})$ measured at 7.18 GHz plotted versus T_c/T for sample S103001. The temperature dependence of R_s below 20 K is shown in the inset. The full lines correspond to an exponential fit with a $\Delta(0)/kT_c$ obtained from penetration depth.

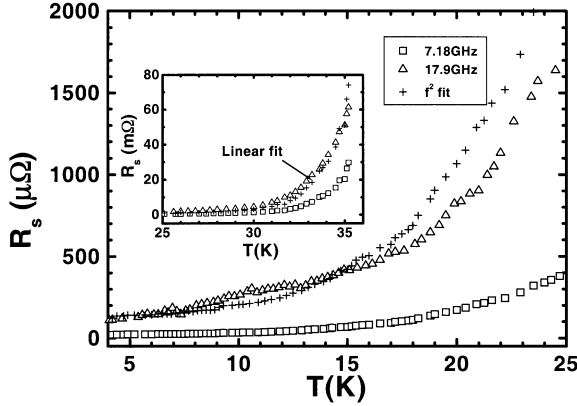


Fig. 4. The temperature dependence of R_s values at 7.18 GHz (open square) and 17.9 GHz (open triangle) for sample S103001. The crosses represent R_s at 17.9 GHz obtained from the values at 7.18 GHz assuming f^2 dependence and, f dependence, however, is assumed in the inset.

However, such a low value is inconsistent with experimental findings by other groups [13], [14].

In summary, a , b -axis penetration depth data do not allow to distinguish between these two models.

IV. SURFACE RESISTANCE MEASUREMENT

Fig. 3 shows the temperature dependence of $R_s(T) - R_s(5\text{ K})$ for sample S103001 at 7.18 GHz. Here the thickness effect has been corrected. The observed linear behavior in this semi-logarithmic plot at low temperature confirm the s-wave symmetry of the order parameter. The full line corresponds to an $\exp(-\Delta/kT)$ behavior with a Δ/kT_c value as determined from the penetration depth data. The inset shows R_s values below 20 K indicating $R_s = 19.4\ \mu\Omega$ at 4.2 K. Frequency scaling according to an assumed square law results in $R_s = 37.6\ \mu\Omega$ at 10 GHz, which is comparable to that of high-quality YBCO thin film. This value is also in accordance with data obtained by the other group [30].

We have also measured a high-order mode ($\text{TE}_{41\delta}$) with a resonant frequency of 17.9 GHz to obtain information about the frequency dependence of R_s (Fig. 4). The frequency depen-

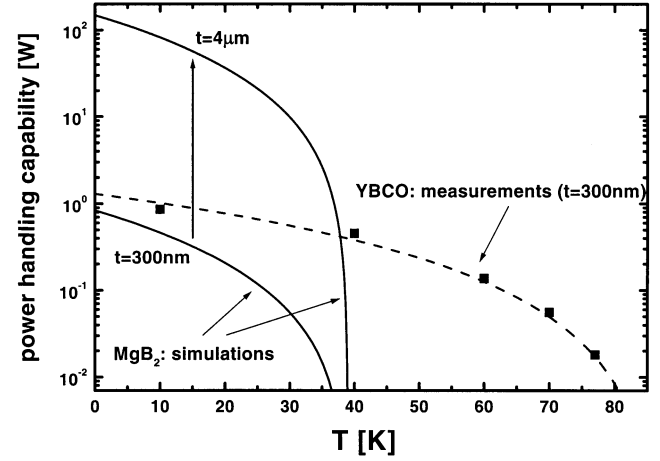


Fig. 5. Comparison of the measured power handling capability of a YBCO coplanar resonator at 1.4 GHz with simulations of a similar device made from MgB₂ based on a model developed in [32]. Taking into account that for MgB₂ the thickness can be increased largely, a higher power handling capability can be expected from MgB₂ coplanar resonator for $T \leq 30\text{ K}$.

dence can be assumed to have a form of f^n , where $n = 2$ is referred to as the square law. For comparison R_s at 7.18 GHz is also plotted. The crosses represent the scaled R_s values at 17.9 GHz obtained from R_s at 7.18 GHz according to a square law. It can be seen that the square law is approximately valid only at very low temperatures up to about 8 K. At high temperatures n increases up to about $n = 1$ for temperatures close to T_c (inset of Fig. 4).

V. POWER HANDLING CAPABILITY

We have shown previously that for epitaxial weak-link free YBCO thin films the power handling capability is ultimately limited by the dc critical current density [31]. Furthermore, it is assumed that in textured MgB₂ weak links do not affect the critical properties due to the larger coherence length of MgB₂ compared to that of HTS material [32]. Therefore, we expect that even for MgB₂ with weak links the power handling capability is determined by the dc critical current density. Fig. 5 shows a comparison of the power handling capability of a YBCO and a MgB₂ coplanar resonator. For the high- T_c material experimental and theoretical values are given, whereas the data for MgB₂ are derived from the model [31] using experimental data for $J_c(0\text{ K}, 0\text{ T}) \approx 10^7\text{ A/cm}^2$ and linear temperature dependence [33]. For YBCO thin films on technical sapphire substrates, the film thickness is usually limited due to the critical thickness to a $t < 300\text{ nm}$ or, using an optimized deposition process [34], $t < 700\text{ nm}$. Taking into account that for textured MgB₂ films large thickness achieved, large microwave power handling capability are expected from MgB₂. This is a direct consequence of the larger coherence length and the larger critical thickness of MgB₂ thin films compared to HTS thin film. Thus, for $T \leq 30\text{ K}$ MgB₂ might be a very promising material for high power microwave applications.

VI. CONCLUSION

By employing advanced dielectric resonator techniques, the microwave surface impedance has been determined for c -axis

oriented MgB₂ thin film. The s-wave nature of order parameter is clearly demonstrated with $\Delta(0)/kT_c$ values around 1.1. The temperature dependence of λ can be well fitted by BCS theory in the entire temperature range below T_c resulting in $\lambda(0)$ values about 100 nm. The temperature dependence of superfluid density ρ_{ab} can be well explained both by an anisotropic one-gap and an isotropic two-gap model. The temperature dependence of R_s at 7.18 GHz shows an exponential behavior below 20 K in accordance with the penetration depth data. The measurement of the frequency dependence of R_s shows that the square law is only valid at low temperatures. For higher temperatures, the exponent of the frequency dependence decreases down to $n = 1$ close to T_c . The R_s values at low temperatures (19.4 $\mu\Omega$ at 4.2 K, 170 $\mu\Omega$ at 20 K and 7.18 GHz) are still dominated by residual losses. The promise for possible cavity applications, e.g., to replace niobium, resides on a dramatic improvement of the residual surface resistance. In turn, the residual surface resistance represents an important figure-of-merit for progress in MgB₂ thin film preparation. Microwave power handling capability simulations show that MgB₂ is also a promising candidate for high power microwave applications compared to HTS when taking lower temperatures of $T \leq 30$ K into account.

REFERENCES

- [1] J. Nagamatsu, N. Nakagawa, T. Muranaka, Y. Zenitani, and J. Akimitsu, "Superconductivity at 39 K in magnesium diboride," *Nature*, vol. 410, p. 63, 2001.
- [2] F. Giubileo, D. Roditchev, W. Sacks, R. Lamy, D. X. Thanh, J. Klein, S. Miraglia, D. Fruchart, J. Marcus, and P. Monod, *Phys. Rev. Lett.*, vol. 87, p. 177 008, 2002.
- [3] P. Seneor, C. T. Chen, N. C. Yeh, R. P. Vasquez, L. D. Bell, C. U. Jung, M.-S. Park, H.-J. Kim, W. N. Kang, and S.-I. Lee, *Phys. Rev. B*, vol. 65, p. 012 505, 2002.
- [4] S. Tsuda, T. Yokoya, T. Kiss, Y. Takano, K. Togano, H. Kito, H. Ihara, and S. Shin, *Phys. Rev. Lett.*, vol. 87, p. 177 006, 2001.
- [5] X. K. Chen, M. J. Konstantinovic, J. C. Irwin, D. D. Lawrie, and J. P. Franck, *Phys. Rev. Lett.*, vol. 87, p. 157 002, 2001.
- [6] F. Bouquet, R. A. Fisher, N. E. Phillips, D. G. Hinks, and J. D. Jorgensen, *Phys. Rev. Lett.*, vol. 87, p. 047 001, 2001.
- [7] J. Kortus, I. I. Mainz, K. D. Belashchenko, V. P. Antropov, and L. L. Boyer, *Phys. Rev. Lett.*, vol. 86, p. 4656, 2001.
- [8] A. Y. Liu, I. I. Mazin, and J. Kortus, *Phys. Rev. Lett.*, vol. 87, p. 087 005, 2001.
- [9] S. Haas and K. Maki, *Phys. Rev. B*, vol. 65, p. 020 502R, 2002.
- [10] A. I. Posazhennikova, T. Dahm, and K. Maki, *Europhysics Lett.*, vol. 60, p. 134, 2002.
- [11] A. A. Golubov, A. Brinkman, O. V. Dolgov, J. Kortus, and O. Jepsen, *Phys. Rev. B*, vol. 66, p. 054 524, 2002.
- [12] A. V. Pronin, A. Pimenov, A. Loidl, and S. I. Krasnosvobodtsev, *Phys. Rev. Lett.*, vol. 87, p. 097 003, 2001.
- [13] G. Lamura, E. D. Gennaro, M. Salluzzo, A. Andreone, J. L. Cochec, A. Gauzzi, C. Cantoni, M. Paranthaman, D. K. Christen, H. M. Christen, G. Giunchi, and S. Ceresara, *Phys. Rev. B*, vol. 65, p. 020 506R, 2002.
- [14] F. Manzano, A. Carrington, N. E. Hussey, S. Lee, A. Yamamoto, and S. Tajima, *Phys. Rev. Lett.*, vol. 88, p. 047 002, 2002.
- [15]
- [16] B. B. Jin, N. Klein, A. Pimenov, A. Loidl, S. I. Krasnosvobodtsev, W. N. Kang, H.-J. Kim, E.-M. Choi, and S.-I. Lee, *Physica C*, vol. 372–376, p. 1283, 2002.
- [17] A. A. Zhukov, A. Purnel, Y. Miyoshi, Y. Bugoslavsky, Z. Lockman, A. Berenov, H. Y. Zhai, H. M. Christen, M. P. Paranthaman, D. H. Lowndes, M. H. Jo, M. G. Blamire, L. Hao, J. Gallop, J. L. MacManus-Driscoll, and L. F. Cohen, *Appl. Phys. Lett.*, vol. 80, p. 2347, 2002.
- [18] A. Andreone, A. Cassinese, C. Cantoni, E. D. Gennaro, G. Lamura, M. G. Maglione, M. Paranthaman, M. Salluzzo, and R. Vaglio, *Physica C*, vol. 372–376, p. 1287, 2002.
- [19] N. Klein, "Electrodynamical Properties of Oxide Superconductors," Juelich Research Center, Internal report Jül-3773, 1997.
- [20] S. S. Hensen, G. G. Müller, C. T. Rieck, and K. Scharnberg, *Phys. Rev. B*, vol. 56, p. 6237, 1997.
- [21] W. N. Hardy, D. A. Bonn, D. C. Morgan, R. X. Liang, and K. Zhang, *Phys. Rev. Lett.*, vol. 70, p. 3999, 1993.
- [22] M. A. Hein, *High-Temperature Superconductor Thin Films at Microwave Frequency*. Springer, Heidelberg: Springer Tracts of Modern Physics, 1999, vol. 155.
- [23] W. N. Kang, H.-J. Kim, E.-M. Choi, C. U. Jung, and S.-I. Lee, *Science*, vol. 292, p. 1521, 2001.
- [24] N. Klein, U. Dähne, U. Poppe, N. Tellmann, K. Urban, S. Orbach, S. Hensen, G. Müllera, and H. Piel, *J. Superconductivity*, vol. 5, p. 195, 1992.
- [25] N. Klein, German Patent DE 42 04 369 C2, 25, 1994.
- [26] N. Klein, H. Chaloupka, G. Müller, S. Orbach, H. Piel, B. Rosa, L. Schultz, U. Klein, and M. Peiniger, *J. Appl. Phys.*, vol. 67, p. 6940, 1990.
- [27] N. Klein, C. Zuccaro, U. Dähne, H. Schulz, N. Tellmann, R. Kutzner, A. G. Zaitsev, and R. Wördenweber, *J. Appl. Phys.*, vol. 78, p. 6683, 1995.
- [28] A. N. Luiren, M. E. Tobar, J. Krupka, R. Woode, E. N. Ivanov, and A. G. Mann, *J. Phys. D: Appl. Phys.*, vol. 31, p. 1383, 1998.
- [29] M. Angst, R. Puzniak, A. Wisniewski, J. Jun, S. M. Kazakov, J. Karpinski, J. Roos, and H. Keller, *Phys. Rev. Lett.*, vol. 88, p. 167 004, 2002.
- [30] M. A. Hein, M. Getta, S. Kreiskott, B. Mönter, H. Piel, D. E. Oates, P. J. Hirst, R. G. Humphreys, H. N. Lee, and S. H. Moon, *Physica C*, vol. 372–376, p. 571, 2002.
- [31] P. Lahl and R. Wördenweber, *Appl. Phys. Lett.*, vol. 81, p. 505, 2002.
- [32] D. Larbalestier, A. Gurevich, D. M. Feldmann, and A. Polyanskii, *Nature*, vol. 414, p. 368, 2001.
- [33] B. Dam, J. M. Huijbregtse, F. C. Klaassen, R. C. F. van der Geest, G. Doornbos, J. H. Rector, A. M. Testa, S. Freisem, J. C. Martinez, B. Stäuble-Pümpin, and R. Griessen, *Nature*, vol. 399, p. 439, 1999.
- [34] R. Wördenweber, J. Einfield, R. Kutzner, A. G. Zaisev, M. A. Hein, T. Kaiser, and G. Müller, *IEEE Trans. On Appl. Supercond.*, vol. 9, pp. 2486–2489, 1999.